



Submitted to

---

**International Europhysics Conference on High Energy Physics, EPS03**, July 17-23, 2003, Aachen  
(Abstract **109** Parallel Session **4**)

**XXI International Symposium on Lepton and Photon Interactions, LP03**, August 11-16, 2003, Fermilab

---

[www-h1.desy.de/h1/www/publications/conf/conf\\_list.html](http://www-h1.desy.de/h1/www/publications/conf/conf_list.html)

# Forward Jet production at HERA

## H1 Collaboration

### Abstract

New parton dynamics, characterized by an initial state cascade which is non-ordered in parton virtuality, is expected to become important in the kinematic region of small Bjorken- $x_{Bj}$ . Evidence for this feature of QCD is searched for by studying events with a forward jet produced close to the direction of the incoming proton in the angular range  $7^\circ < \theta_{jet} < 20^\circ$ . The measurements are compared with the predictions of simulations assuming ordered or non-ordered emissions in the initial state cascade. The cross section for forward jet production is presented as a function of  $x_{Bj}$ , and shows a significant deviation to the predictions based on DGLAP evolution. We also present the forward jet cross section as a function of the energy fraction the forward jet takes from the initial proton, and as a function of the transverse momentum of the forward jet.

# 1 Introduction

HERA has extended the available  $x_{Bj}$  region down to values of  $x_{Bj} > 10^{-5}$ , for values of the momentum transfer,  $Q^2$ , larger than a few GeV, where perturbative calculations in QCD are still expected to be valid. In Deep Inelastic Scattering (DIS) a parton in the proton can induce a QCD cascade consisting of several subsequent parton emissions, before the final parton interacts with the virtual photon.

Several different prescriptions of the QCD dynamics at small values of  $x_{Bj}$  have been proposed. These include QCD parton evolution schemes such as the DGLAP [1, 2, 3, 4] evolution equation, the small  $x_{Bj}$  specific BFKL [5, 6, 7] evolution equation as well as the CCFM [8, 9, 10, 11] evolution equation, which forms a bridge between DGLAP and BFKL using the concept of color coherence.

Differences between the different dynamical approaches to the parton cascade are expected to be most prominent in the phase space region towards the proton remnant direction, i.e. away from the scattered quark.

We investigate the parton evolution at small values of  $x_{Bj}$  using jet production in the forward angular region (close to the proton remnant direction) in the laboratory frame. The analysis presented here is based on 5 times more statistics than our published one [12] and is complementary to a similar analysis [13] which used high energetic pions instead of jets. A schematic diagram for forward jet production is shown if Fig 1.

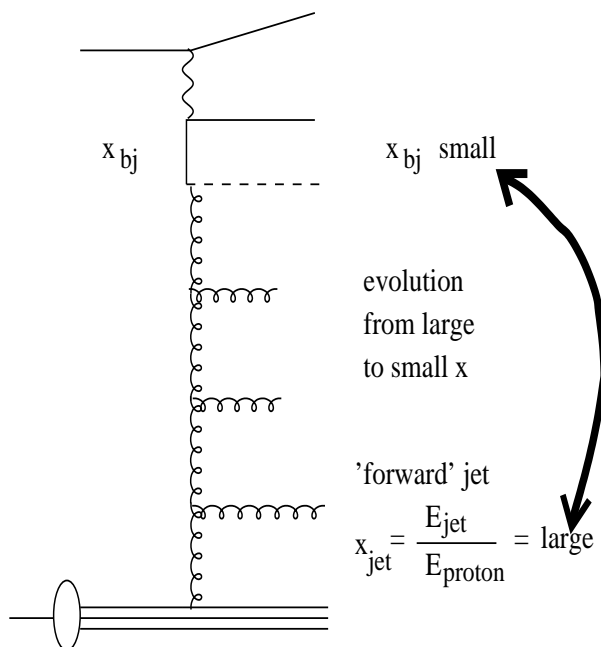


Figure 1: Schematic diagram for forward jet production at HERA. The evolution from large  $x_{jet}$  to small  $x_{Bj}$  is indicated. The phase space for DGLAP evolution in  $Q^2$  is restricted by the requirement of  $p_{t,jet}^2 \sim Q^2$ .

In the DGLAP evolution scheme, the virtualities  $k_i$  of the propagator gluons are strictly increasing from the proton to the photon. Thus the cross section for forward jet production with  $p_{t\,jet}^2 \sim Q^2$  is expected to be small, since there is no phase space left for further parton radiation between the forward jet and the virtual photon. In the BFKL description, however, the virtualities (and transverse momenta)  $k_{\perp i}$  can perform a so-called random walk. Based on calculations in the LLA of the BFKL kernel, the cross section for DIS events at low  $x_{Bj}$  and large  $Q^2$  with a high  $p_{t\,jet}^2$  jet in the proton direction (a forward jet) [14, 15] is expected to rise more rapidly with decreasing  $x_{Bj}$  than expected from DGLAP based calculations.

## 2 Data and analysis method

The region in which the forward jet measurement is performed is chosen such that the phase space for jet production according to the DGLAP evolution is suppressed compared to that available for the BFKL evolution. This is achieved by requiring  $p_{t\,jet}^2 \sim Q^2$ , where  $p_{t\,jet}^2$  is the transverse momentum squared of the forward jet. In addition the momentum fraction of the forward jet  $x_{jet} = E_{jet}/E_p$  is required to be large, whereas  $x_{Bj}$  is kept as small as possible, thus enhancing the phase space for evolution in  $x$  while suppressing the evolution in  $Q^2$ .

The  $e^+p$  scattering data have been collected at  $\sqrt{s} = 300$  GeV with the H1 detector in 1997 and correspond to an integrated luminosity of  $13.72$  pb $^{-1}$ .

DIS events are selected by requiring a scattered electron in the backward SPACAL calorimeter with an energy  $E_{e'}$   $> 10$  GeV in the angular range of  $156^\circ < \theta_e < 175^\circ$ . The kinematics are determined from the scattered electron:  $Q^2 = 4E_e E_{e'} \cos^2(\theta_e/2)$  and  $y = 1 - (E_{e'}/E_e) \sin^2(\theta_e/2)$  where  $E_e$  is the incident positron energy. In summary the following cuts are applied:

$$\begin{aligned} E_{e'} &> 10 \text{ GeV} \\ 156^\circ &< \theta_e < 175^\circ \\ 0.1 &< y < 0.7 \\ 5 \text{ GeV}^2 &< Q^2 < 75 \text{ GeV}^2 \end{aligned}$$

The forward jets are defined using the  $k_t$ -jet algorithm [16, 17] in its inclusive mode (applied in the Breit-frame) by requiring:

$$\begin{aligned} p_{t\,jet} &> 3.5 \text{ GeV} \\ 7.0^\circ &< \theta_{jet} < 20.0^\circ \\ x_{jet} &> 0.035 \\ 0.5 &< p_{t\,jet}^2/Q^2 < 2 \end{aligned}$$

where  $p_{t\,jet}$  is measured in the laboratory frame.

The RAPGAP [18] Monte Carlo model uses LO matrix elements supplemented with initial and final state DGLAP parton showers (DIR-model). In addition resolved virtual photon processes can be included (RES-model). In the following RAPGAP will be labeled as RG. The

# H1 Forward Jet Data

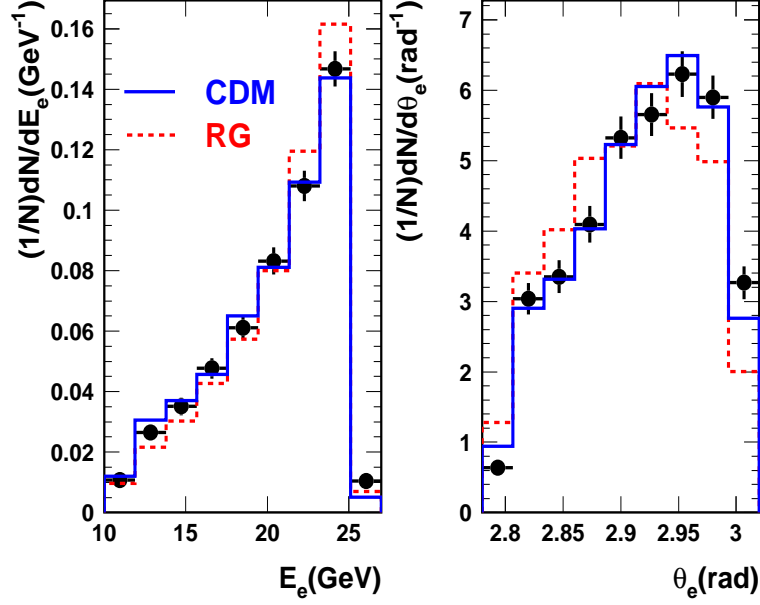


Figure 2: *Distribution of the energy  $E_e$  and the angle  $\Theta_e$  of the scattered electron variables after the forward jet selection. The solid (dashed) line shows the predictions from CDM (RG) Monte Carlo after full detector simulation.*

DJANGO [19] Monte Carlo model is used together with the Color-Dipole-Model as implemented in ARIADNE [20] for higher order QCD radiation, labeled as CDM. Simulated events of the RG-DIR and CDM Monte Carlo programs have been processed through the detailed H1 detector simulation. In Fig. 2 the normalized distributions of the scattered electron energy and scattering angle, after the forward jet selection, are shown. In Fig. 3 the normalized distributions of basic jet variables, after the forward jet selection, are compared to the Monte Carlo predictions. In both Figs. 2 and 3 good agreement of the data with the full detector simulation of the CDM MC is observed. The RG Monte Carlo shows deviations to the data, as expected from a pure DGLAP type prediction. In Fig. 4 we show the transverse energy flow around the axis of the selected forward jet as a function of  $\Delta\eta = \eta_{jet} - \eta_{clus}$  and  $\Delta\phi = \phi_{jet} - \phi_{clus}$  in a slice of  $|\Delta\phi| = 1$  and  $|\Delta\eta| = 1$ , respectively. Also shown are the predictions from the Monte Carlo simulations.

The CDM Monte Carlo, which describes best the data at detector level, is used for correcting the data to hadron level. The difference of the correction factors obtained by the two Monte Carlos, CDM and RG is  $\sim 8\%$ , and is treated as systematic error.

The effects of initial state QED radiation are corrected for using HERACLES interfaced to DJANGO and RAPGAP.

The following systematic errors are considered:

# H1 Forward Jet Data

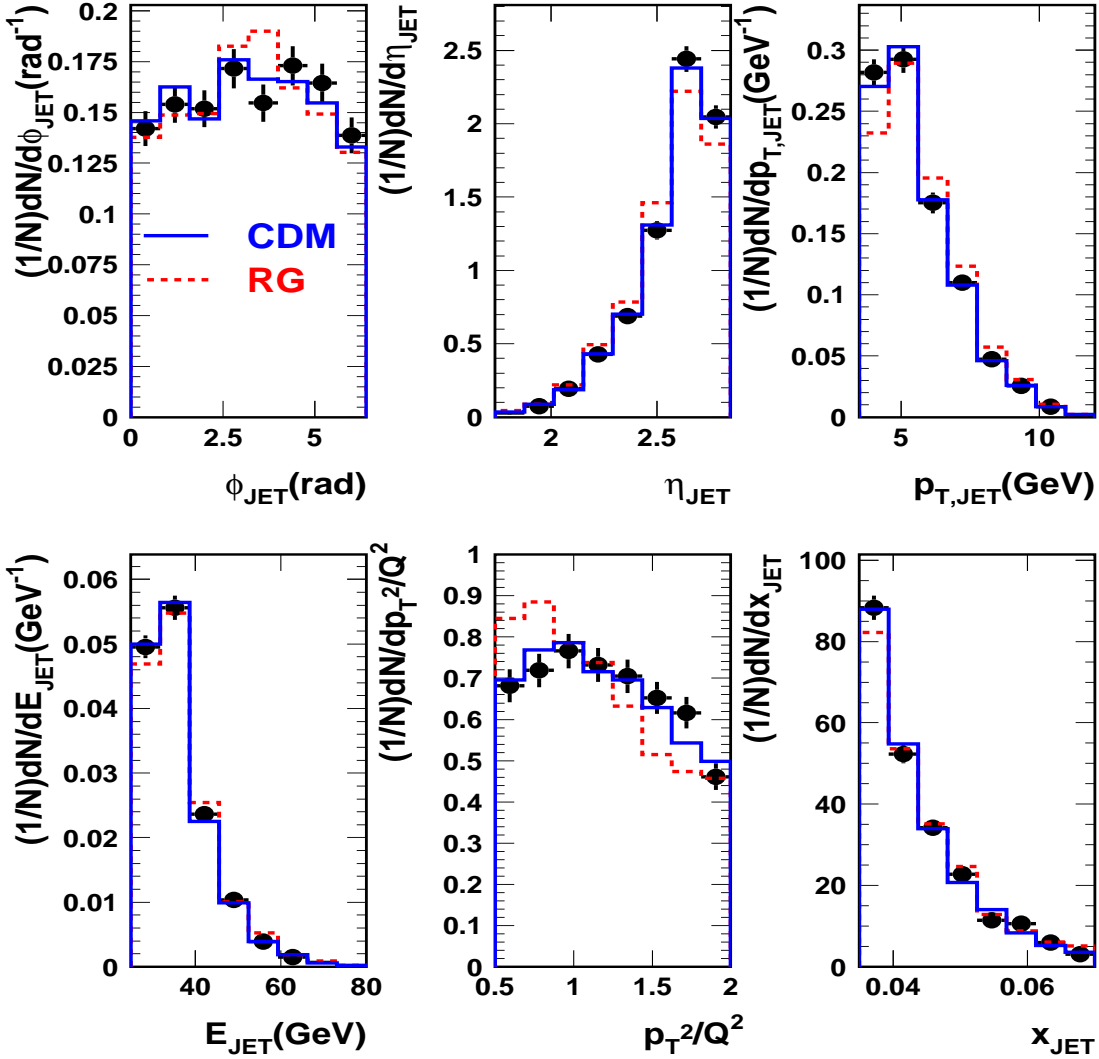


Figure 3: *Distribution of basic jet variables after the forward jet selection. The solid (dashed) line shows the predictions from CDM (RG) Monte Carlo after full detector simulation.*

- The error on the hadronic energy scale of 4 % in the LAr- Calorimeter results in an error of the cross section measurement of  $\sim 6\%$ .
- The error on the electromagnetic energy scale of 1 % of the SPACAL Calorimeter results in an error of the cross section measurement of  $\sim 3\%$ .
- An error of 1 mrad is assumed on the angle measurement of the scattered electron, resulting in an error of the cross section measurement of  $\sim 3\%$ .
- The error coming from the model dependence between RG and CDM of  $\sim 8\%$ .

## H1 Forward Jet Data

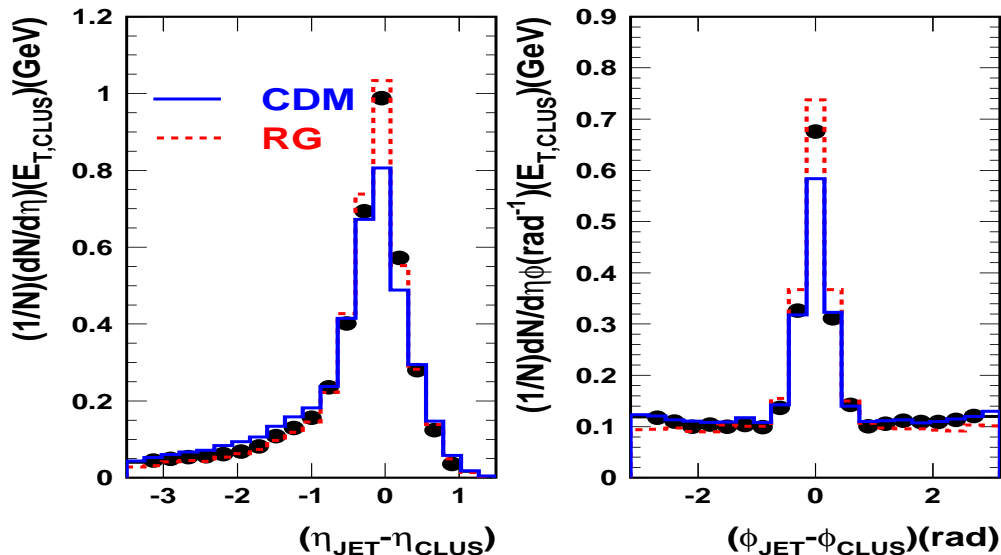


Figure 4: Transverse energy flow around the axis of the selected forward jet as a function of  $\Delta\eta = \eta_{jet} - \eta_{clus}$  and  $\Delta\phi = \phi_{jet} - \phi_{clus}$  in a slice of  $|\Delta\phi| = 1$  and  $|\Delta\eta| = 1$ , respectively. Also shown are the predictions from the CDM (solid) and RG (dashed) Monte Carlo simulations.

- The photoproduction background is estimated using the PHOJET [21, 22] Monte Carlo simulations to  $\sim 1\%$ .

In Fig. 5-7 we show the forward jet cross section as a function of  $x_{Bj}$ ,  $x_{jet}$  and  $p_{t,jet}$  for  $p_{t,jet} > 3.5$  GeV and  $p_{t,jet} > 5$  GeV corrected to the hadron level. Also shown are the predictions from a pure DGLAP type Monte Carlo (RG - DIR), including also a contribution from resolved virtual photons (DIR+RES), and a simulation using the Color Dipole Model (CDM) as implemented in ARIADNE (DJANGO). In ARIADNE the parton emissions perform a random walk in transverse momentum leading to a situation similar to the one expected in BFKL. Whereas the DGLAP type prediction falls below the data at small  $x_{Bj}$ , CDM and DGLAP including resolved virtual photons give a good description of the measurement. The CASCADE implementation of the CCFM evolution equation, which is based on  $k_t$ -factorization, overestimates the data.

### 3 Conclusion

A new measurement of the forward jet production cross section as a function of  $x_{Bj}$ ,  $x_{jet}$  and  $p_{t,jet}$  has been performed using an integrated luminosity of  $13.72 \text{ pb}^{-1}$ . The data are up to a factor of two larger than the predicted cross section based on  $\mathcal{O}(\alpha_s)$  and QCD calculation in the collinear factorization ansatz (DGLAP).

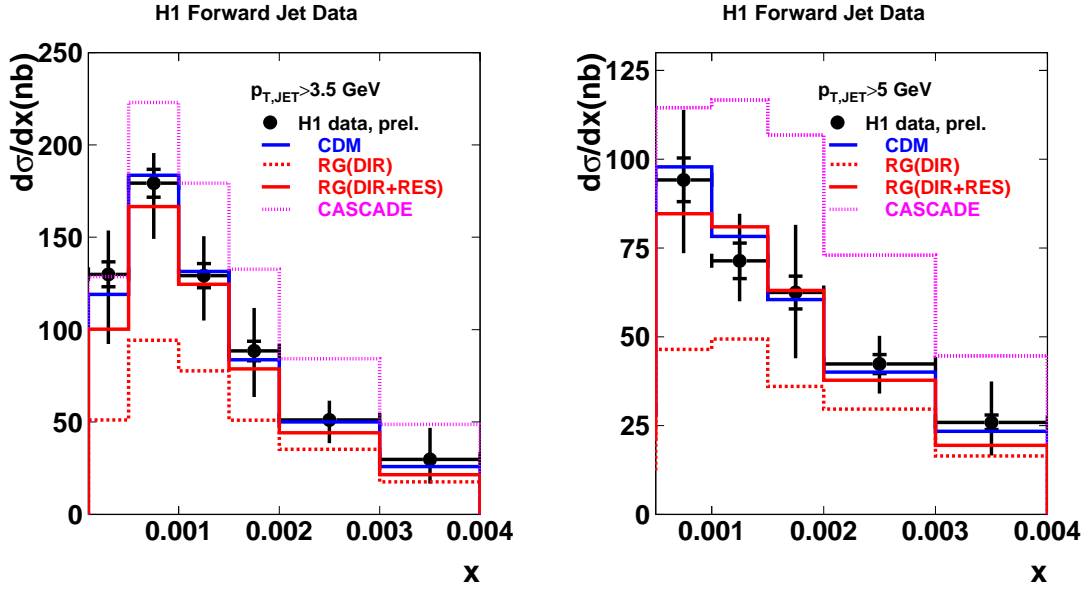


Figure 5: The cross section for forward jet production on hadron level, as a function of  $x_{Bj}$  for  $p_{t,jet} > 3.5$  GeV (left) and  $p_{t,jet} > 5$  GeV (right). Also shown are the predictions from the CDM, RG and CASCADE Monte Carlos.

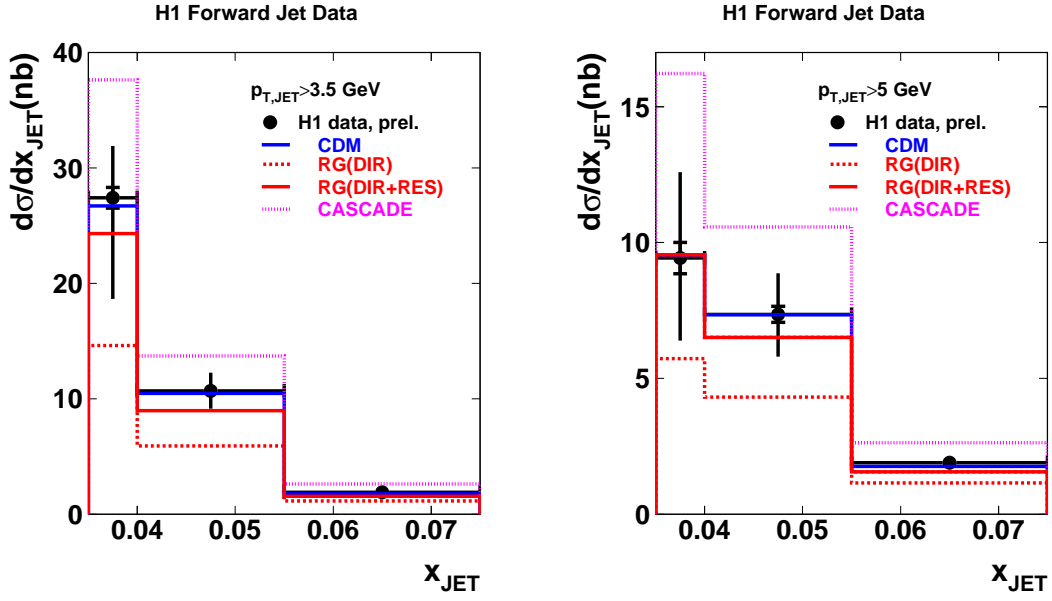


Figure 6: The cross section for forward jet production on hadron level, as a function of  $x_{jet}$  for  $p_{t,jet} > 3.5$  GeV (left) and  $p_{t,jet} > 5$  GeV (right). Also shown are the predictions from the CDM, RG and CASCADE Monte Carlos.

Using a hadron level Monte Carlo model incorporating resolved virtual photon processes in addition to the usual direct photon processes, the data are reasonably well described. Also

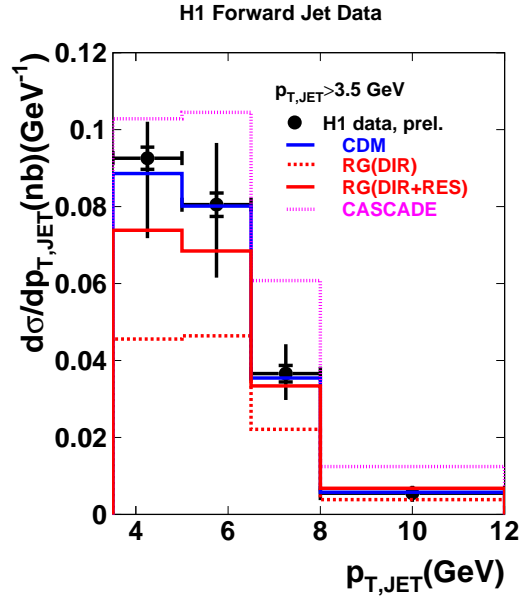


Figure 7: The cross section for forward jet production on hadron level, as a function of  $p_{t \text{ jet}}$  for  $p_{t \text{ jet}} > 3.5 \text{ GeV}$  (left) and  $p_{t \text{ jet}} > 5 \text{ GeV}$  (right). Also shown are the predictions from the CDM, RG and CASCADE Monte Carlos.

the Color Dipole Model, which simulates higher order QCD radiation without strong ordering of the transverse momenta of the emitted partons, describes the measurements well. The more sophisticated CCFM approach, which is based on angular ordering coming from color coherence, predicts too high a rate of forward jet events.

## References

- [1] V. Gribov, L. Lipatov, *Sov. J. Nucl. Phys.* **15** (1972) 438 and 675.
- [2] L. Lipatov, *Sov. J. Nucl. Phys.* **20** (1975) 94.
- [3] G. Altarelli, G. Parisi, *Nucl. Phys.* **B 126** (1977) 298.
- [4] Y. Dokshitzer, *Sov. Phys. JETP* **46** (1977) 641.
- [5] E. Kuraev, L. Lipatov, V. Fadin, *Sov. Phys. JETP* **44** (1976) 443.
- [6] E. Kuraev, L. Lipatov, V. Fadin, *Sov. Phys. JETP* **45** (1977) 199.

- [7] Y. Balitskii, L. Lipatov, *Sov. J. Nucl. Phys.* **28** (1978) 822.
- [8] M. Ciafaloni, *Nucl. Phys.* **B 296** (1988) 49.
- [9] S. Catani, F. Fiorani, G. Marchesini, *Phys. Lett.* **B 234** (1990) 339.
- [10] S. Catani, F. Fiorani, G. Marchesini, *Nucl. Phys.* **B 336** (1990) 18.
- [11] G. Marchesini, *Nucl. Phys.* **B 445** (1995) 49.
- [12] H1 Collaboration, C. Adloff et al., *Nucl. Phys.* **B 538** (1999) 3.
- [13] H1 Collaboration, Forward  $\pi^0$  meson production at HERA, Lidia Goerlich - talk presented at DIS 2002, April, 2002.
- [14] A. Mueller, *Nucl. Phys.* **B (Proc. Suppl) 18C** (1990) 125.
- [15] A. Mueller, *J. Phys.* **G 17** (1991) 1443.
- [16] S. Catani, Y. Dokshitzer, M. Seymour, B. Webber, *Nucl. Phys.* **B 406** (1993) 187.
- [17] S. Catani, Y. Dokshitzer, B. Webber, *Phys. Lett.* **B 285** (1992) 291.
- [18] H. Jung, *The RAPGAP Monte Carlo for Deep Inelastic Scattering, version 2.08*, Lund University, 2002, <http://www.quark.lu.se/~hannes/rapgap/>.
- [19] G. A. Schuler, H. Spiesberger, , in \*Hamburg 1991, Proceedings, Physics at HERA, vol. 3\* 1419-1432. (see HIGH ENERGY PHYSICS INDEX 30 (1992) No. 12988).
- [20] L. Lönnblad, *Comp. Phys. Comm.* **71** (1992) 15.
- [21] R. Engel, *Z. Phys.* **C66** (1995) 203.
- [22] R. Engel, J. Ranft, *Phys. Rev.* **D54** (1996) 4244, hep-ph/9509373.